Process integration and development of inverted photonic crystal arrays

M. Tinker[a)]
Erik Jonsson School of Engineering and Computer Science, Mail Station EC 33, University of Texas at Dallas, Richardson, Texas 75083-0688

E. Schonbrun
Department of Electrical and Computer Engineering, Campus Box 425, University of Colorado, Boulder, Colorado 80309-0425

J.-B. Lee
Erik Jonsson School of Engineering and Computer Science, Mail Station EC 33, University of Texas at Dallas, Richardson, Texas 75083-0688

W. Park
Department of Electrical and Computer Engineering, Campus Box 425, University of Colorado, Boulder, Colorado 80309-0425

(Received 22 September 2005; accepted 30 January 2006; published 9 March 2006)

A processing technology has been developed to produce inverted two-dimensional photonic crystal structures by embedding an array of silicon pillars inside a polyimide matrix and releasing this structure from the underlying substrate. The spatial distribution of the high dielectric and low dielectric regions of these structures is inverted compared to the spatial distribution of standard photonic crystal structures produced by etching air holes in a high dielectric slab. Consequently these structures are far more difficult to fabricate. The integration requirements required for developing this technology are discussed along with the processing technology developed to fabricate these devices. An inverted photonic crystal device based on the superprism effect was successfully demonstrated. © *2006 American Vacuum Society.* [DOI: 10.1116/1.2180254]

I. INTRODUCTION

Two-dimensional (2D) photonic crystals have typically been developed by etching a systematic array of air holes in a thin slab of a high-index semiconductor such as silicon or GaAs. The dielectric contrast between the air holes and the semiconductor slab generates a distinct band gap within the photonic crystal that can be used to generate many interesting devices. The semiconductor slabs used to make these devices are first patterned, then reactive-ion etched, and then finally released to produce the requisite structures. In some device geometries, the devices are not even released. Consequently, the processing technology used to generate these devices is dependent on only a few processing steps that can be readily integrated to produce the necessary structures. This greatly facilitates product development and a whole variety of different device geometries have been manufactured by using this relatively straightforward technology.[1–8]

However, the early theoretical literature indicated that two-dimensional photonic crystals could also be developed from an array of high dielectric rods suspended inside a low dielectric matrix. In effect the spatial distribution of the dielectric regions in these photonic crystals is inverted compared to the dielectric distribution of more standard photonic crystal devices developed by etching air holes in a dielectric slab. This can offer significant advantages. Firstly, since these structures can be readily produced by using a low-index polymer film for the matrix, they can be mechanically stretched by microelectromechanical system (MEMS) actuators to alter the geometry of the device to produce active optical devices.[9] In addition, since light within these structures exhibits a markedly different electrical and magnetic field distribution inside the array, these structures also offer the potential for generating photonic crystal devices with useful geometries and improved optical characteristics. For example, inverted photonic crystals can be used to generate waveguides with 90° bends with relatively high band widths not possible with standard devices.[10–12]

Although a large number of experimental studies have been reported on photonic crystal devices generated by etching air holes in high dielectric slabs,[1–8] very few experimental studies have been reported on photonic crystals made by suspending high dielectric rods in a low dielectric matrix. The studies on inverted photonic crystal structures reported to date have been generated by etching tall high-index pillars directly on top of an underlying substrate.[13–16] However, it is extremely difficult to constrain light to the photonic crystal slab in the vertical direction in these systems. Consequently, these geometries are highly susceptible to the leakage of light out of the plane of the device. This has been the primary factor limiting the active development of these devices.

Better optical confinement could be achieved by forming a photonic crystal slab from a thin polymer film and then releasing the structure from the underlying substrate. The light can then be confined in the vertical direction by total internal reflection. In addition, these devices can also be readily actuated mechanically. However, this morphology is

[a)]Electronic mail: mark.tinker@comcast.net

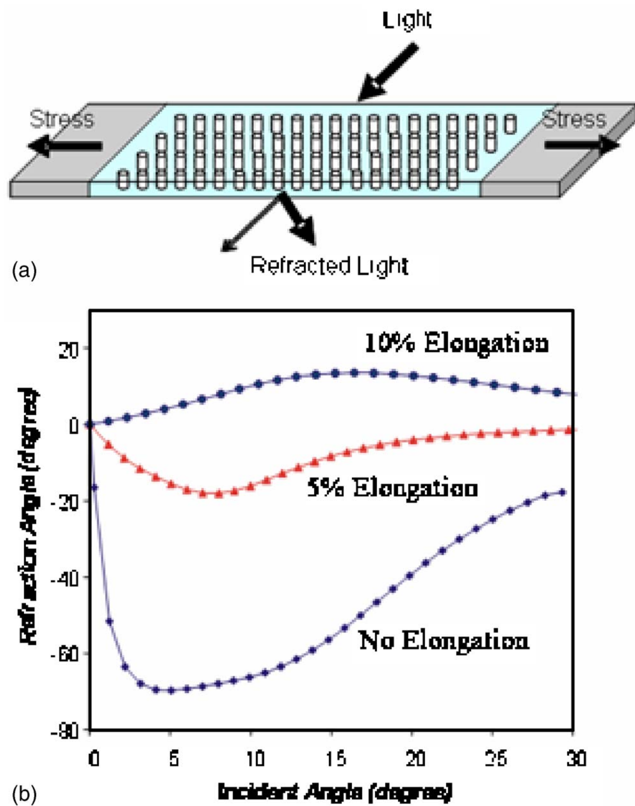

FIG. 1. (a) Design concept of dynamically tunable two-dimensional flexible photonic crystal device and (b) refraction angle vs elongation (Ref. 9).

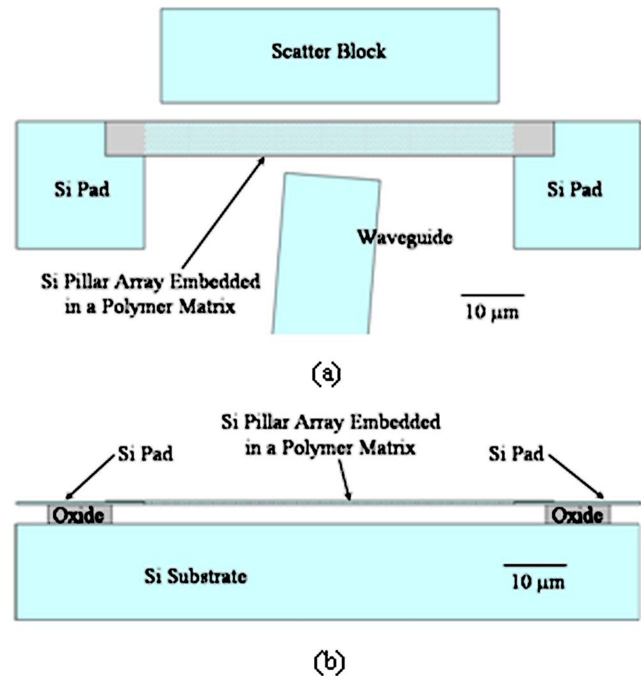

FIG. 2. (a) Photonic crystal layout and (b) device cross section.

exceedingly difficult to fabricate and to date no such study has been reported on this type of device in the literature.

Recently a process was developed in order to generate a suspended inverted photonic crystal array for a proposed MEMS beam steering device based on the superprism effect and negative refraction.[9,17] This process is discussed below.

II. PROCESS DEVELOPMENT

A. Proposed device and process concepts

A simplified schematic of the proposed beam steering device is shown in Fig. 1(a). The device, designed for 1.55 μm infrared light, is composed of a triangular lattice of silicon pillars suspended in a polymer matrix with a lattice spacing equal to 600 nm, a pillar diameter equal to 360 nm, and a pillar height equal to 350 nm. Thermal actuators attached to the ends of this array can potentially stretch the matrix by up to several percent. Simulations reveal that this can strongly modify the dispersion surface of the device and markedly change the direction of outgoing light by the superprism effect as shown in Fig. 1(b). When unstressed, simulations reveal that the photonic crystal refracts light at an extremely large, negative angle by up to $\sim$70°. If the photonic crystal is then uniformly stretched between 5% and 10%, the refraction angle decreases dramatically, changing the direction of the outgoing light.[9]

A process to generate an inverted photonic crystal array, however, first had to be developed and demonstrated prior to any implementation of an active device. The basic concept of this process first involves generating a photonic crystal array of high-index silicon rods on top of thermal oxide using an anisotropic reactive-ion etch. These rods can then be encased in a thin polymer matrix by spin coating a polymer over the array, the matrix patterned by reactive-ion etch, and the array released from the underlying substrate by undercutting the entire matrix with buffered oxide etch (BOE). The actual implementation and demonstration of this process are described below.

B. Test layout

The general layout of the test configuration used to evaluate the inverted photonic crystal array used to confirm the device technology is shown in Fig. 2(a). The 2D array designed to test the device was composed of 10 rows by 100 columns with a lattice spacing of 615 nm, a pillar diameter of 400 nm, and a pillar height equal to 350 nm. This array was encased in a polymer matrix extending approximately 100 nm above and below the array. The polymer matrix was also extended several microns beyond the ends of the photonic crystal array in order to suspend the photonic crystal from the two large silicon pads situated at the ends of the array once it is released. A cross section of the suspended device is shown in Fig. 2(b).

An angled waveguide shown at the bottom of Fig. 2(a) is used to direct light into the photonic crystal array at the desired angle of incidence. The photonic crystal array has been designed to refract the light out of the plane of the array and into an objective lens positioned above the device in order to directly observe the path of the light inside the pho-

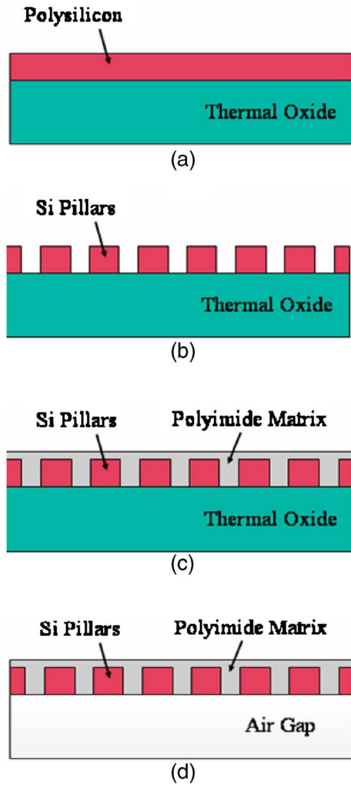

FIG. 3. Process flow: (a) Polysilicon LPCVD on thermal oxide, (b) silicon CF_4/O_2 RIE of silicon pillars and Cr etch, (c) polyimide deposition, and (d) BOE oxide release of photonic crystal array.

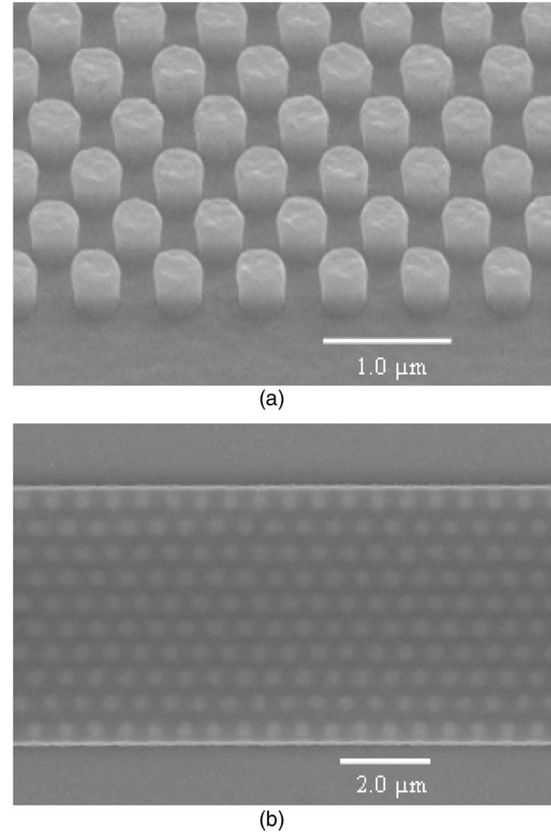

FIG. 4. SEM micrographs: (a) tilted view of etched silicon pillars and (b) triangular array of silicon pillars embedded in patterned polyimide.

tonic crystal itself. A large silicon block has also been placed above the photonic crystal to scatter any light exiting from the array into the objective lens above the device in order to detect the location of the outgoing light.

C. Integration requirements

The superprism effect is particularly sensitive to small changes in dimension. Consequently, the average lattice spacing and pillar diameter of the photonic crystal arrays should be controlled to within 615 nm±1% and 400 nm±5%, respectively, in order to effectively control the direction of the outgoing light. The etch profiles should also be highly anisotropic in order to avoid excessive variations in the shape of the pillars.

Planarity of the device is also an important consideration. The anisotropic etch used to form the silicon pillars must be stopped within approximately 20 nm after hitting the underlying thermal oxide to avoid any excessive variations in the planarity of the polymer matrix across the bottom of the array caused by overetching the underlying oxide. Since planarity across the top of the device was achieved by flowing a polymer over the top of the silicon pillar array during spin coating, the polymer should also be fluid enough to achieve good planarization across the top of the array. The thickness of this polymer should also be limited to approximately 100 nm above the top of the array in order to limit any adverse optical effects. Implementation of large scale devices, however, will almost certainly require planarization of the device by chemical mechanical polish.

Finally, the polymer used to support the silicon pillar array must also meet several requirements. First the polymer must be transparent to light near the telecommunication wavelength of 1.55 μm and must also exhibit a refractive index of around 1.50 in order to create a photonic crystal with a highly dispersive medium conducive to strongly refracting light. In addition, the polymer must exhibit good gap fill between adjacent pillars in order to avoid the development of air holes which could have an adverse effect on the optical performance. The polymer must also be resistant to the buffered oxide etch used to release the device. In particular, the interface between the polymer and the silicon must be resistant to attack. Furthermore, residual stresses generated in the polymer during processing should not seriously deform the matrix during subsequent release. In addition, the polymer must be rigid enough to withstand any stiction forces generated during release but also capable of being elongated elastically up to a few to several percent during actuation. Finally the polymer should be creep resistant. Polyimide was ultimately chosen as the matrix material for this application after extensive evaluation.[18–20]

D. Process description

The process technology developed for producing an inverted photonic crystal device is shown schematically in Fig.

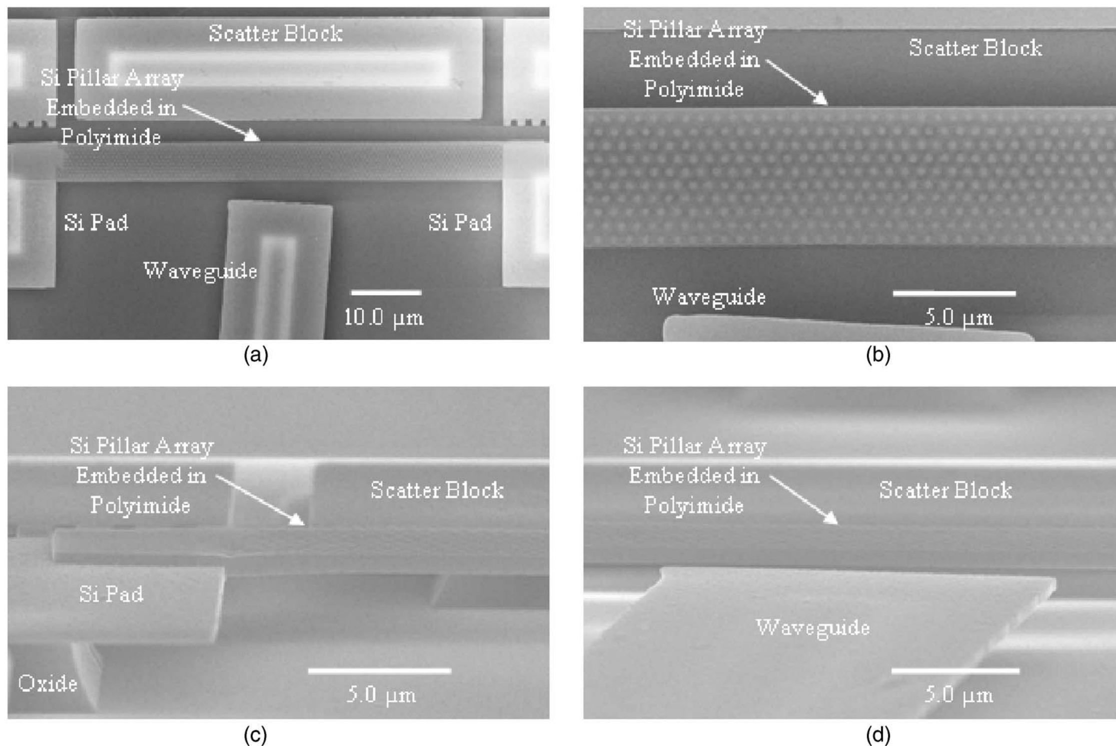

FIG. 5. (a) Low magnification SEM image and (b) higher magnification image at 0° tilt showing suspended photonic crystal device; high tilt SEM images at 80° tilt showing (c) polyimide attached to polysilicon pad and (d) embedded silicon pillar array suspended directly in front of the waveguide.

3(a) through Fig. 3(d). Polysilicon is first deposited to a thickness of 350 nm by low-pressure chemical-vapor deposition (LPCVD) on top of a 3.0-μm-thick thermal oxide as shown in Fig. 3(a). A bilayer polymethyl methacrylate (PMMA) and copolymer resist stack was then e-beam exposed to form the resist pattern for the photonic crystal array used for subsequent lift-off. A 15-nm-thick chromium mask was then formed by lift-off and the silicon pillars reactive-ion etched by using a $CF_4/8.75\% O_2$ plasma. The reactive-ion etch (RIE) generates a highly anisotropic etch profile and stops abruptly on the underlying oxide. The Cr caps were then removed by using a highly selective Cr etch. The resultant silicon pillar array is shown in Fig. 3(b).

Polyimide was then spin coated over the silicon pillars and baked at 350 °C for 30 min in nitrogen to form a 450-nm-thick polymer matrix film as shown in Fig. 3(c). The polyimide pattern was then formed using the same lift-off process used for the silicon pillars and the matrix anisotropically etched using a 100% O_2 reactive-ion etch. The device was released using a standard BOE methanol release process. The completed device is depicted in Fig. 3(d).

E. Device characterization

A high magnification of a scanning electron microscopy (SEM) micrograph of a silicon pillar array tilted to 45° is shown in Fig. 4(a). Note the nearly vertical sidewalls formed during etching and the abrupt manner in which the silicon etch has been stopped on the underlying oxide. The lattice spacing and average pillar diameter measured across several different arrays measured 615 nm$\pm$1% and 400 nm$\pm$5%, respectively, close to the desired specifications. The SEM micrograph in Fig. 4(b) also shows a high magnification of a typical silicon pillar array embedded in a polyimide matrix at 0° tilt. The edge of the polyimide matrix is aligned to within 100 nm of the edge of the array. The polyimide matrix appears smooth and exhibits no noticeable evidence of voiding.

Figure 5(a) shows a low magnification SEM micrograph of the suspended photonic crystal structure after BOE etch at 0° tilt. The waveguide, silicon pads, and scatter block are only partially undercut during etch and are still supported by the underlying oxide. However, the photonic crystal has been totally undercut by the buffered oxide etch and is now suspended at its ends by direct contact of the polyimide to the two large silicon pads. A higher magnification of the suspended microstructure is also shown in Fig. 5(b). The array appears totally intact and exhibits no noticeable evidence of chemical attack. No deformation or distortion of the array is evident. The high tilt SEM micrographs shown in Figs. 5(c) and 5(d) clearly confirm that the silicon pillar array has been totally undercut and suspended at its ends by direct contact of the polyimide to the polysilicon pads. Note that the photonic crystal exhibits no noticeable sagging or any other form of deformation along the entire length of the device.

III. OPTICAL CHARACTERIZATION

The optical characterization process involves collecting and imaging light scattered normal to the device surface. The device was tested by projecting transverse-electric (TE) light

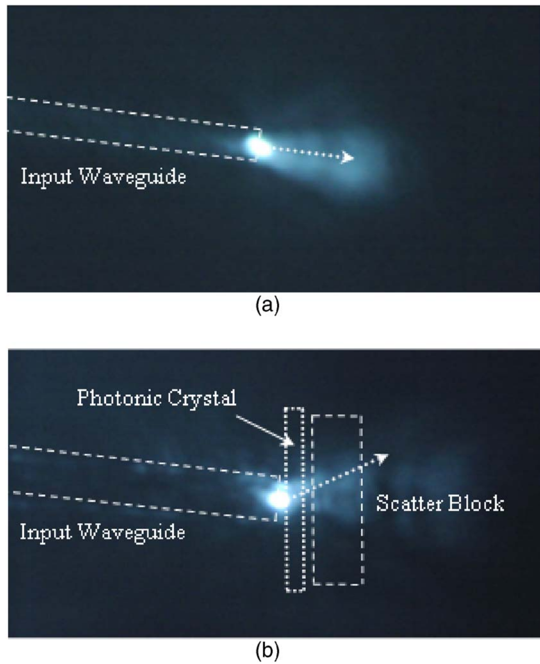

FIG. 6. Experimentally collected images of light scattered from the photonic crystal device where (a) shows the direction of the light emitted from the input waveguide and (b) shows the direction of the light refracted through the photonic crystal from light incident at 8°. The arrows indicate the direction of light propagation simulated numerically. The locations of the input waveguide, the photonic crystal, and the scattering block have been highlighted in the micrographs.

at 1546 nm through a waveguide angled at an 8° angle of incidence to the photonic crystal. Light exiting from the waveguide with no intervening test structure placed in the path of the light travels directly parallel to the direction of the waveguide as shown in Fig. 6(a). However, light refracted through a photonic crystal placed directly in the path of the light as shown in Fig. 6(b) bends past the normal of the photonic crystal towards the upper right at an angle greater than the incident wave, clearly demonstrating both the superprism effect and negative refraction. The light then diffracts off the scattering block after exiting the array. The simulated angle of refraction calculated for the photonic crystal dimensions used in the test structure is shown by the direction of the arrow in the micrograph. The actual angle of refraction detected in the photonic crystal appears somewhat larger than that for the simulation. This is most likely a consequence of the extreme sensitivity of the superprism effect to small variations in the device dimensions.

IV. CONCLUSIONS

A processing technology has been developed for producing inverted photonic crystal arrays by releasing a thin silicon pillar array embedded inside a polyimide matrix from the underlying substrate. The basic processing technology developed for producing an inverted photonic crystal structure was described along with the various processing and integration requirements needed to successfully implement a working device. A passive device was designed, developed, and demonstrated for an inverted photonic crystal array being employed in a beam steering device based upon the superprism effect.

ACKNOWLEDGMENT

The authors gratefully acknowledge the financial support from the National Science Foundation through Grant No. ECS-0304442.

[1]Y. A. Vlasov, N. Moll, and S. J. McNab, J. Appl. Phys. **95**, 4538 (2004).
[2]S. J. McNab, N. Moll, and Y. A. Vlasov, Opt. Express **11**, 2927 (2003).
[3]Y. Sugimoto, N. Ikeda, N. Carlsson, K. Asakawa, N. Kawai, and K. Inoue, IEEE J. Quantum Electron. **38**, 760 (2002).
[4]S. Y. Lin, E. Chow, J. Bur, S. G. Johnson, and J. D. Joannopoulos, Opt. Lett. **27**, 1400 (2002).
[5]M. Tokushima, H. Kosaka, A. Tomita, and H. Yamada, Appl. Phys. Lett. **76**, 952 (2000).
[6]M. Loncar, D. Nedeljkovic, T. Doll, J. Vuckovic, A. Scherer, and T. P. Pearsall, Appl. Phys. Lett. **77**, 1937 (2000).
[7]M. Notomi, A. Shinya, K. Yamada, J. Takahashi, C. Takahashi, and I. Yokohama, IEEE J. Quantum Electron. **38**, 736 (2002).
[8]S. Y. Lin, E. Chow, S. G. Johnson, and J. D. Joannopoulos, Opt. Lett. **25**, 1297 (2000).
[9]W. Park and J.-B. Lee, Appl. Phys. Lett. **85**, 4845 (2004).
[10]J. D. Joannopoulos, R. D. Meade, and J. N. Winn, *Photonic Crystals: Molding the Flow of Light* (Princeton University Press, Princeton, NJ, 1995), Chap. 5, p. 54.
[11]A. Mekis, J. C. Chen, I. Kurland, S. Fan, P. R. Villeneuve, and J. D. Joannopoulos, Phys. Rev. Lett. **77**, 3787 (1996).
[12]S. G. Johnson, P. R. Villeneuve, S. Fan, and J. D. Joannopoulus, Phys. Rev. B **62**, 8212 (2000).
[13]S. Assefa *et al.*, Appl. Phys. Lett. **85**, 6110 (2004).
[14]M. Tokushima, H. Yamada, and Y. Arakawa, Appl. Phys. Lett. **84**, 4298 (2004).
[15]V. Poborchii, T. Tada, T. Kanayama, and A. Moroz, Appl. Phys. Lett. **82**, 508 (2003).
[16]V. V. Poborchii, T. Tada, and T. Kanayama, Opt. Commun. **210**, 285 (2002).
[17]E. Schonbrun, M. Tinker, W. Park, and J. B. Lee, IEEE Photonics Technol. Lett. **17**, 1196 (2005).
[18]H.-G. Kim, Y.-M. An, D.-K. Moon, and J.-G. Park, Jpn. J. Appl. Phys., Part 1 **39**, 1085 (2000).
[19]P. A. Kawka and R. O. Buckius, Int. J. Thermophys. **22**, 517 (2001).
[20]M. Saito, T. Gojo, Y. Kato, and M. Miyagi, Infrared Phys. Technol. **36**, 1125 (1995).